NIH Public Access
Author Manuscript
Exp Cell Res. Author manuscript; available in PMC 2009 November 1.

Published in final edited form as:
Exp Cell Res. 2008 November 1; 314(18): 3415–3425. doi:10.1016/j.yexcr.2008.08.020.

Cellular Localization of the Activated EGFR Determines Its Effect on Cell Growth in MDA-MB-468 Cells

Dustin C. Hyatt and **Brian P. Ceresa**
Department of Cell Biology, University of Oklahoma Health Sciences Center, Oklahoma City, Oklahoma 73190

Abstract

The epidermal growth factor (EGF) receptor (EGFR) is a ubiquitously expressed receptor tyrosine kinase that regulates diverse cell functions that are dependent upon cell type, the presence of downstream effectors, and receptor density. In addition to activating biochemical pathways, ligand stimulation causes the EGFR to enter the cell via clathrin-coated pits. Endocytic trafficking influences receptor signaling by controlling the duration of EGFR phosphorylation and coordinating the receptor's association with downstream effectors. To better understand the individual contributions of cell surface and cytosolic EGFRs on cell physiology, we used EGF that was conjugated to 900 nm polystyrene beads (EGF-beads). EGF-beads can stimulate the EGFR and retain the activated receptor at the plasma membrane. In MDA-MB-468 cells, a breast cancer cell line that over-expresses the EGFR, only internalized, activated EGFRs stimulate caspase-3 and induce cell death. Conversely, signaling cascades triggered from activated EGFR retained at the cell surface inhibit caspase-3 and promote cell proliferation. Thus, through endocytosis, the activated EGFR can differentially regulate cell growth in MDA-MB-468 cells.

Keywords

EGFR; endocytosis; caspase-3; apoptosis

Introduction

The epidermal growth factor receptor (EGFR) is the prototypical receptor tyrosine kinase. It is a transmembrane protein with approximately equal portions of the receptor localized outside and inside the cell. Ligands, such epidermal growth factor (EGF), bind to the extracellular domain of the receptor and induce a conformational change in the receptor that allows two receptors to dimerize. Ligand binding also activates the EGFR's intrinsic kinase domain resulting in transphosphorylation of carboxyl terminal tyrosine residues on the receptor's binding partner. The phosphotyrosines serve as docking sites for the src homology 2 (SH2) domains of downstream signaling molecules, such as phosphatidyl inositol 3'kinase (PI3K) and phospholipase Cγ (PLCγ), or adaptor proteins, like Grb2 or SHC [1,2]. The coordinated activation of these pathways regulates cell growth, differentiation, migration, proliferation, and

Correspondence to: Brian P. Ceresa.

Address Correspondence to: Brian P. Ceresa, Department of Cell Biology, University of Oklahoma Health Sciences Center, 940 Stanton L. Young Blvd, Oklahoma City, Oklahoma 73190 Tel: 405-271-2377 Fax: 405-271-3548 Email: brian-ceresa@ouhsc.edu.

Publisher's Disclaimer: This is a PDF file of an unedited manuscript that has been accepted for publication. As a service to our customers we are providing this early version of the manuscript. The manuscript will undergo copyediting, typesetting, and review of the resulting proof before it is published in its final citable form. Please note that during the production process errors may be discovered which could affect the content, and all legal disclaimers that apply to the journal pertain.

NIH-PA Author Manuscript
NIH-PA Author Manuscript
NIH-PA Author Manuscript

NIH-PA Author Manuscript

NIH-PA Author Manuscript

NIH-PA Author Manuscript

apoptosis. These cellular changes are critical to proper tissue development, regeneration, and homeostasis.

One way that EGFR signaling is regulated is via the endocytic pathway. In addition to biochemical responses, ligand binding also triggers the internalization of the ligand:receptor complex via clathrin-mediated endocytosis. Entry into the endocytic pathway ultimately results in lysosomal degradation of the receptor [3,4] and serves to control receptor signaling. The duration of receptor activation is controlled by the kinetics of membrane trafficking; the receptor's proximity to downstream effectors is dictated by the spatial localization within the endocytic pathway [5,6]. It has been demonstrated by numerous groups that disrupting the temporal and spatial regulation of the EGFR results in aberrant signaling [7,8]. Despite numerous biochemical studies that point to endocytosis-dependent differences in the magnitude and efficiency of receptor:effector communication, there are little data to indicate physiological consequences of inhibiting receptor internalization.

Limitations in understanding the spatial regulation of EGFR signaling reflect the shortcomings of the tools used to block receptor internalization. Approaches that use either dominant negative proteins or RNA interference (RNAi) require that either the dominant negative construct is expressed or the protein is knocked down for significant periods of time. This temporal constraint introduces the possibility of compensatory mechanisms arising, such as receptor up-regulation or alterations in the steady-state distribution of the receptor as the cell attempts to maintain homeostasis [9-11]. Alternatively, some inhibitors of endocytic trafficking, both pharmacologic and biochemical, can be non-specific and disrupt multiple endocytic trafficking events [12,13]. This complicates the interpretation of EGFR-specific effects. Finally, many of the approaches do not permit for adequate distinction between changes in duration of receptor activity and spatial placement of the receptor.

In order to overcome these limitations, we have employed an EGFR-specific ligand that prevents internalization of the EGFR, without disrupting the internalization of other proteins. By using MDA-MB-468 cells that express high levels of EGFRs, have slowed endocytic trafficking, and exhibit no appreciable EGFR degradation over time, we can compare the functional significance of EGFR localization and avoid the complications of varying levels of activated receptor.

Although EGFR activity has been well documented as promoting cell growth and differentiation, it is well established that in some cells, activation of the EGFR causes cell death. This has been reported in MDA-MB-468 cells and A431 cells [14-16]. A common characteristic of these cells is that they overexpress the EGFR - a feature that is reasonable to predict that would enhance cell growth. Knowing how the same receptor can promote both cell growth and apoptosis is important in understanding the molecular regulation of EGFR signaling. Further, identifying the how to transition EGFR signaling from pro-growth to pro-apoptosis has therapeutic potential for the treatment of cancers that overexpress the EGFR.

In this study, we restricted EGFR signaling to the plasma membrane utilizing EGF covalently conjugated to 900 nm polystyrene beads (“EGF-beads”). The EGF-beads are able to stimulate the EGFR upon binding, but the associated bead is too large to internalize through the clathrin-coated pit (50-100 nm in diameter) and is retained at the cell surface. We have found that despite comparable levels of phosphorylation of internalized and cell surface EGFR, only the intracellular EGFR can induce caspase-3-mediated apoptosis. Thus, the intracellular localization of the activated EGFR can forecast its activity.

NIH-PA Author Manuscript

NIH-PA Author Manuscript

NIH-PA Author Manuscript

Materials and methods

Cell Culture—MDA-MB-468, HeLa, and A431 cells were obtained from ATCC. MDA-MB-468 and A431 cells were maintained in Dulbecco's Modified Eagle's Medium (DMEM) (Gibco) supplemented with 10% Fetal Bovine Serum, 100 units/ml penicillin, 100 units/ml streptomycin, and 2 mM glutamine at 37°C in 5% CO_2. HeLa cells were maintained in DMEM supplemented with 5% Fetal Bovine Serum, 100 units/ml penicillin, 100 units/ml streptomycin, and 2 mM glutamine at 37°C in 5% CO_2.

EGF-Bead Synthesis—Human recombinant Epidermal Growth Factor (lnvitrogen, Carlsbad, CA) was covalently conjugated to 0.9 mm diameter carboxylate modified polystyrene beads (Sigma, St. Louis, MO) as described previously [17].

Ligand Treatment, cell lysate preparation, and immunoblotting—Sub-confluent dishes of MDA-MB-468 cells were incubated with the indicated concentrations of EGF or EGF-beads in DMEM at 37°C. Ligand incubation was terminated by washing the cells two times with room temperature PBS pH 7.3 and equilibrating the cells to 4°C. Cell lysates were prepared on ice by solubilizing cells in 4°C lysis buffer (150 mM NaCl, 1% Nonidet P-40, 0.5% deoxycholate, 0.1 % SDS, 50 mM Tris, pH 8.0, 10 mM sodium pyrophosphate, 100 mM sodium fluoride, and 2 mM phenylmethylsulfonyl fluoride). Equivalent amounts of protein were immunoblotted using antibodies against the EGFR (SC-03, Santa Cruz Biotechnology, Santa Cruz, CA), phosphotyrosine (PY99, Santa Cruz Biotechnology, Santa Cruz, CA), phosphoEGFR (pTyr 1068, Cell Signaling, Danvers, MA), α-actin (Sigma, St. Louis , MO) followed by probing with a horseradish peroxidase-conjugated goat anti-mouse or goat anti-rabbit secondary antibody (Pierce, Rockford, IL). Detected proteins were visualized by enhanced chemiluminescence (ECL) on the UV Products Imaging System.

Trypsin protection assay—Epidermal Growth Factor Receptor internalization was determined by trypsin resistance [18]. MDA-MB-468 cells were incubated in serum-free DMEM for 2 hours, subjected to 5 mM EDTA/PBS and collected. Equal numbers of cells (300,000) were incubated with EGF or EGF-Beads for the indicated periods of time at 37°C. After treatment, the cells were washed twice and incubated on ice for 3 min with ice-cold, acidified DMEM (pH 4.0) containing 1 % bovine serum albumin. The cells were washed with ice-cold PBS and incubated with trypsin (1 mg/ml in PBS [pH 7.4]) at 4°C for 30 minutes with end over end rotation. The reaction was stopped by the addition of soybean trypsin inhibitor (10 mg/ml), 2 mM N-ethylmaleimide (Sigma, St. Louis, MO), and 2 mM phenylmethylsulfonyl fluoride (Sigma, St. Louis, MO). In parallel, mock treated cells were incubated with the stopping solution for 30 min. Cell lysates were collected then probed by immunoblot with an anti- phosphotyrosine antibody (PY99, Santa Cruz Biotechnology, Santa Cruz, CA), anti-transferrin receptor (Cell Signaling, Danvers, MA), or anti-α-tubulin (Sigma, St. Louis, MO).

Indirect immunofluorescence—Cells were processed as described previously [19]. The phosphorylated EGFR was detected with a mouse monoclonal phospho-EGF Receptor (Tyr1068) antibody (Cell Signaling, Danvers, MA) according to manufacturer's instructions. Alexa488 conjugated goat anti-mouse was purchased from Molecular Probes. Images were collected using a Leica TCS NT confocal microscope.

[^{3}H] Thymidine Incorporation—Subconfluent MDA-MB-468 cells were serum starved for 6 hours, followed by 16 hours of incubation in DMEM (0 ng/ml EGF), 10% FBS, EGF, or EGF-Beads (~1×10^9)in media containing 1 μCi [^{3}H] -thymidine (20.0 Ci/mmol, Perkin Elmer), 100 units/ml penicillin, and 100 units/ml streptomycin. The cells were washed three times with ice-cold PBS and incubated with 0.5 ml of ice-cold 10% trichloroacetic acid for 1 hour. The acid insoluble fraction was solubilized in 0.5 ml of .1 % SDS, and the wells were

NIH-PA Author Manuscript

NIH-PA Author Manuscript

NIH-PA Author Manuscript

rinsed one time with an additional 0.25 ml of 0.1 % SDS. The rinses were pooled, and [^{3}H]-thymidine incorporation was determined by scintillation counting [18]. Under basal conditions (DMEM treated cells), [^{3}H]-thymidine incorporation was 5,000 - 10,000 cpm.

In experiments that examined the effect of caspase-3 inhibition, cells were pretreated for one hour with 10 mM DEVD-CHO (Calbiochem, San Diego, CA) prior to stimulation. DEVD-CHO inhibited EGF-stimulated caspase-3 activity by 80% (data not shown).

Caspase-3 Assay—4×10^5 MDA-MB-468 cells were plated in a 35 mm dish. Serum starved cells were treated as indicated for 16 hours. The amount of caspase-3 activity was measured using the EnzCheck® Caspase-3 Kit #2 from Molecular Probes (Eugene, OR) according to the manufacture's protocol. Briefly, caspase-3 activity is measured as a function of the cleavage of the rhodamine 110-derived substrate zDEVD-R110. This substrate is a non-fluorescent bis-amide that is first converted by caspase-3 to the mono-amide and then to the bright, green-fluorescent rhodamine 110 (excitation/emission maxima ~496/520 nm). Fluorescent activity was measured using a BMG Labtech's NOVOstar Microplate Fluorimeter.

[^{125}I]-EGF degradation—Cells were incubated for 7.5 minutes with [^{125}I]-EGF (Perkin Elmer) (1ng/ml) at 37°C in binding buffer (DMEM /20 mM HEPES/ 0.1 % bovine serum albumin, pH 7.3). Cells were washed four times on ice with ice cold PBS to remove external, unbound [^{125}I]-EGF. Pre-warmed, 37°C media was added to the cells and they were returned to 37°C for the indicated periods of time. At each time point, the media was collected. The remaining cells were solubilized in 1 % NP-40/ 20 mM Tris pH 7.4. Cell lysates were incubated with 10% trichloroacetic acid and 1% BSA as a carrier protein on ice for 1 hour. Intact protein was separated from degraded by centrifugation for 15 minutes at 14,000 rpm in an Ependorf Microfuge at 4°C. The radioactivity in each fraction (secreted, intact, degraded) was determined using Beckman Gamma Counter [20]. The percentage of intact [^{125}I]-EGF was calculated as a function of the total radioactivity.

[^{125}I]-EGF Internalization—MDA-MB-468 cells were equilibrated to 4°C on ice and incubated with 0.5 ml [^{125}I]-EGF(Perkin Elmer) at specific activity of 50,000 cpm/ng and a concentration of 10 ng/ml for 2 hours on ice in washing media (DMEM, 20 mM HEPES pH 7.4, 0.1 % BSA). Free radioligand was removed with two washes in ice-cold PBS, and then incubated at 37°C with pre-warmed washing media for the indicated times. After 37°C incubation, cells were washed twice with ice cold PBS, followed by two washes (8 minutes) in 0.75 ml of 0.2 M acetic acid pH 2.8/0.5 M NaCl. Washes were pooled and counted. Cells were solubilized with 0.75 ml of 1M NaOH and collected to count. Radioactivity was measured using a Beckman 5500B Gamma counter [21].

[^{125}I]-Transferrin internalization—Following pre-treatment for 1 hour with DMEM, 100 ng/ml EGF, or 1×10^9 EGF-beads/ml, media was removed and replaced with 37°C binding media containing 180 nMol [^{125}I]-transferrin (0.7 μCi/mg, Perkin Elmer). Cells were placed at 37°C for the indicated times. Following incubation, free and cell-surface associated [^{125}I]-Tfn were removed as described for [^{125}I]-EGF. Cells were solubilized in 1 M NaOH and the associated radioactivity was measured using a Beckman 5500B Gamma counter [18].

DNA fragmentation assays—MDA-MB-468 cells were treated overnight as indicated. Cells were collected, pelleted by centrifugation at 800 × g for 5 minutes and resuspended in 10 mM NaCl, 10 mM Tris pH 7.5,10 mM EDTA pH 8.0. The cells were supplemented with 0.5% SDS and 0.2 mg/ml proteinase K and incubated for 2 hours at 50°C. Following tris-phenol/chloroform/isoamylalcohol (25:24:1) and chloroform/isoamylalcohol (24: 1) extraction, the DNA was precipitated, resuspended in 10 mM Tris/1 mM EDTA pH 8.0 with

NIH-PA Author Manuscript

NIH-PA Author Manuscript

NIH-PA Author Manuscript

1 mg/ml RNase A for 1 hour at 37°C. DNA (15 μg) was separated on a 1.2% agarose gel in 0.5 × TBE (25 mM Tris base/25 mM boric acid/0.5 mM EDTA) [22].

MTT Assay—Cells were plated as a density of 5,000 cells/well of a 96-well dish for 24 hours. Cells were incubated 0-100 ng/ml EGF, or 5% FBS for 72 hours then assayed using MTT (3, [4,5-dimethylthiazol-2-yl]-2,5-diphenyltetrazolium bromide) assay [23]. Data are plotted as the ratio of cells under the described treatment, relative to the number of cells in serum-free media. Statistics were calculated using Prism software (GraphPad Software, Inc, San Diego, CA).

Cell Counting—Cells were plated in 60 mm dishes at a density of 800,000 cells/dish. Cells were incubated 0-100 ng/ml EGF, or 5% FBS for 72 hours. Cells were collecting in 1 ml volume, counted using a hemacytometer, and plotted relative to cell grown in DMEM.

Results

MDA-MB-468 cells are a human mammary epithelial cell line. Treatment of these cells with EGF causes the cells to undergo apoptosis as seen by the dose dependent decrease in cell number, cell viability, and DNA fragmentation (Figure 1). EGF-dependent apoptosis is seen by changes in cell morphology (Figure 5A) and decreased [^{3}H]-thymidine incorporation (Figure 5B). This finding is consistent with what has been reported by other [14,16]. However, it remains unclear why EGFR stimulation causes cell growth in some cells and apoptosis in others.

A common feature of cell lines, like MDA-MB-468 cells, that undergo apoptosis in response to EGF is that they express high levels of EGFRs [14,15]. The physiological density of EGFRs is 50,000 -100,000 receptors/cell. Much higher levels of EGFRs are seen in cells lines that undergo EGF-dependent apoptosis, i.e. MDA-MB-468 cells (~ 1.3×10^6 EGFRs/cell [24]) and A431 cells (~1.5 ×106 EGFRs/cell) [25].

Many cells that overexpress the EGFR have slowed ligand-stimulated EGFR degradation [26,27]. To determine if this was the case for MDA-MB-468 cells, we quantitated the internalization of the radiolabeled EGF and the degradation of the EGF:EGFR complex. For these studies, HeLa cells serve as positive control for rapid EGFR endocytic trafficking when physiological levels of EGFRs (~50,000 EGFRs/cell) are expressed. However, we are aware of the numerous differences between MDA-MB-468 and HeLa cells.

Internalization of ^{125}I-EGF can occur in MDA-MB-468 cells although the kinetics of endocytosis are slower as compared to HeLa cells (Figure 2A). In contrast, there is very little radioligand degradation and ligand-stimulated EGFR degradation in MDA-MB-468 cells (Figure 2B-D). In fact, in MDA-MB-468 cells 16 hours of EGF stimulation does not produce appreciable degradation of the EGFR (Figure 3B and Figure 8). This rate of degradation is dramatically different from what we observe in HeLa cells and what has been reported in HepG2 cells [28].

Since in MDA-MB-468 cells EGF stimulation causes the receptor to internalize, but not degrade, we hypothesized that the intracellular accumulation of the activated EGFR causes apoptosis. If this hypothesis is correct, then active EGFRs at the plasma membrane would not induce cell death, whereas those inside the cell would.

To test this hypothesis, we have employed an EGFR-specific ligand that prevents internalization of the EGFR, without disrupting the endocytosis of other proteins. We restricted EGFR signaling to the plasma membrane utilizing EGF covalently conjugated to 900 nm

NIH-PA Author Manuscript

NIH-PA Author Manuscript

NIH-PA Author Manuscript

polystyrene beads (subsequently referred to as “EGF-beads”) as described in Experimental Procedures. This ligand can activate the EGFR and retain it at the cell surface. EGF-beads are specific for the EGFR and do not require pre-treatment of the cells that could allow compensatory processes to occur. EGF-beads have been used previously in single cell assays to measure receptor activation [17,29] and actin assembly [30].

To verify that our EGF-beads function as proposed, MDA-MB-468 cells were stimulated with EGF or EGF-beads and the resulting cell lysates were immunoblotted with anti-phosphoEGFR (pTyr 1068) and anti-phosphotyrosine antibodies (Figure 3A). Both treatments yielded a concentration-dependent increase in EGFR phosphorylation. Cells treated with polystyrene beads without conjugated EGF (Beads) did not induce EGFR phosphorylation above background. Importantly, cells were also treated with the final wash in our EGF-beads synthesis (Wash). The inability of the final wash to induce EGFR phosphorylation indicates there are not appreciable levels of free EGF remaining in our EGF-bead preparation. An analysis of longer periods of stimulation with EGF and EGF-beads indicates that activation of the EGFR can be sustained for up to 16 hours (Figure 3B).

To determine whether the active EGFR is receptor is retained at the cell surface, we used indirect immunofluorescence to examine the localization of the phosphorylated (active) EGFR. Following treatment with EGF or EGF-beads for 1-16 hours, cells were fixed, and probed by indirect immunofluorescence using a phospho-EGFR antibody (pTyr 1068, Cell Signaling) and an Alexa488 goat-anti-mouse secondary antibody (Molecular Probes). Brightfield images of these same cells were collected as well. Representative images from 1,4, and 16 hours post treatment are shown in Figure 4A. Treatment with EGF causes the activated EGFR to redistribute to endosomes (1 and 4 hour time points). The distribution of the activated EGFR following 16 hours of EGF treatment is concentrated in the cell and reflects that fact that MDA-MB-468 cells undergo apoptosis following EGF treatment for 16 hours. In contrast, cells that had been treated with EGF-beads, the majority of activated EGFR accumulated at the cell surface.

These data indicate there is a clear difference in the steady-state distribution of the activated EGFR following EGF versus EGF-bead treatment. However, these results do not discount the possibility that receptors stimulated with soluble EGF are able to recycle from endosomes and back to the plasma membrane for reactivation.

The immunofluorescence data are supported by a biochemical assay that demonstrates the EGF, but not EGF-beads, removes the active EGFR from the cell surface (Figure 4B). The trypsin protection assay monitors receptor internalization by examining the phosphorylated receptors in an intact cell that are resistant to cleavage by trypsin following ligand stimulation. Receptors on the cell surface will be cleaved, whereas those that are internalized will be protected from trypsinization. There is a time-dependent increase in the amount of protected, phosphorylated EGFR with EGF treatment as detected by anti-phosphotyrosine antibodies. Incubation with EGF-beads does not protect the EGFR from trypsinization, indicating the receptor is retained on the cell surface. As a control to validate the effectiveness of trypsinization, we have monitored the cleavage of the transferrin receptor (TfnR). The transferrin receptor continually recycles from the plasma membrane to the cell surface, so a portion of the total receptor population is always resistant to trypsinization. Nevertheless, there is a reduction in the amount of immunoreactive transferrin receptor at 150 kDa and an accumulation of cleavage products following trypsinization as compared to those cells that were not subjected to trypsinization.

Importantly, EGF-beads do not inhibit all clathrin-mediated endocytosis. Cells were maintained in DMEM alone or supplemented with EGF or EGF-beads for 1 hour and assayed

NIH-PA Author Manuscript

NIH-PA Author Manuscript

NIH-PA Author Manuscript

for internalization of the transferrin receptor using [^{125}I]-transferrin (Figure 4C). The transferrin receptor, like the EGFR, is internalized via clathrin-coated pits. The rates of [^{125}I]-transferrin internalization were indistinguishable in cells maintained in DMEM alone or supplemented with EGF or EGF-beads. Thus, EGF-beads can activate the cell surface EGFRs and retain them on the cell surface, but do not inhibit the clathrin-mediated endocytosis of other cell surface proteins.

Cell surface EGFRs promote cell growth

Having verified that the EGF-beads function as predicted, we examined how EGFR-modulated cell physiology is affected when the receptor is restricted to the plasma membrane. The concentration of EGF-beads chosen for this assay, and all subsequent assays, was empirically determined to be the amount that can stimulate EGFR phosphorylation to a level that is comparable to 100 ng/ml of EGF. In our first experiment, we treated MDA-MB-468 cells with either EGF or EGF-beads and monitored the cells (Figure 5A). As a control, cells maintained either in media alone (0 ng/ml EGF) or media supplemented with 5% fetal bovine serum (Serum). Under both conditions, cells exhibited no gross morphological differences. Cells treated with EGF-beads had a similar morphology, although it is slightly obscured by the presence of the EGF-beads. In contrast, cells treated with EGF exhibited a rounded morphology that is characteristic of cells undergoing apoptosis.

To better quantify this EGFR-mediated response, MDA-MB-468 cells were treated with DMEM, EGF-beads, EGF, or Fetal Bovine Serum (FBS) and assayed for [^{3}H]-thymidine incorporation (Figure 5B) as a measure of cell growth and viability. When the incorporation of [^{3}H]-thymidine was measured, treatment with EGF-beads caused an ~4-fold increase in [^{3}H]-thymidine incorporation as compared to 50% reduction in the EGF-treated cells (Figure 5B). Similar trends in DNA synthesis were seen in A431 cells, another cell line that overexpresses the EGFR (~1.5×10^{6} EGFRs/cell) and undergoes apoptosis in response to EGF [31]. While treatment of A431 cells with EGF-beads caused similar increase in [^{3}H]-thymidine incorporation, the response was not as robust as what was seen in MDA-MB-468 cells (Supplemental Data, Figure 1).

As a second assay to examine these differences in receptor signaling, we examined caspase-3 activity. Caspase-3 is regarded as an “executioner caspase”, meaning once it becomes activated the cell has committed itself to an apoptotic fate. Cells treated with soluble EGF were able to induce caspase-3 activity, indicating that the rounded morphology of cells following EGF treatment was coincident with induction of an apoptotic pathway (Figure 6). As predicted by the enhanced level of [^{3}H]-thymidine incorporation, treatment with EGF-beads failed to activate caspase-3 (Figure 6). In fact, cells treated with EGF-beads had reduced caspase-3 activity. Using three different assays, we were able to demonstrate the inverse effects of EGF and EGF-bead stimulation.

We next wanted to determine if intracellular EGFRs could promote cell growth, but it was being masked by the induction of apoptosis. To determine if this was the case, we assayed [^{3}H]-thymidine incorporation in cells in which caspase-3 was pharmacologically inhibited with DEVD-CHO (Calbiochem). In MDA-MB-468 cells, DEVD-CHO was able to inhibit EGF-stimulated caspase-3 activity 80% (data not shown). Cells treated with the caspase-3 inhibitor DEVD-CHO had levels of [^{3}H]-thymidine incorporation that were statistically indistinguishable from unstimulated cells (Figure 7). Treatment with soluble EGF fails to mediate apoptosis, but does not increase DNA synthesis as compared to untreated cells. EGF-bead treatment of cells with or without DEVD-CHO had no effect on [^{3}H]-thymidine incorporation. Thus, the EGFR in MDA-MB-468 cells mediates cell death through a combination of inducing pro-apoptotic and removing pro-growth signals.

NIH-PA Author Manuscript

NIH-PA Author Manuscript

NIH-PA Author Manuscript

Based on our observations regarding the kinetics of EGFR trafficking, we predict that after 16 hours of EGF stimulation, the EGFR has sustained activity and there are significant amounts of activated EGFR within the cell. To test this prediction, cells were stimulated with either EGF or EGF-beads for 16 hours and assayed for receptor phosphorylation (Figure 8). As expected, EGF-bead treatment resulted in receptor phosphorylation that was sustained at 16 hours. Cells stimulated with high concentrations of EGF (100 ng/ml) had a level of receptor phosphorylation and total EGFR that was comparable to those treated with the EGF-beads. In cells treated with 1 ng/ml or 10 ng/ml EGF, the level of phosphorylated EGFR was only slightly higher than basal levels. The limited receptor phosphorylation after 16 hours of EGF (as compared to 1 hour treatment, Figure 1A) is likely the result of consumption of the EGF as there is a molar excess of EGFRs as compared to EGF at those concentrations [32]. Consistent with our observed kinetics of receptor trafficking, treatment with high concentrations of EGF resulted in the accumulation of activated the EGFR after 16 hours. Since the levels of EGFR phosphorylation are comparable for EGF and EGF-beads stimulation, the duration of EGFR phosphorylation does not factor into our interpretation of the differences in signaling in response to EGF and EGF-beads.

Discussion

Despite the fact that overexpression of the EGFR and its related family members is associated with many cancers and poor prognosis for survival [33], the ability of EGF to stimulate apoptosis in cells expressing high levels of EGFR is well-established. Until now, it has been unclear how the same receptor can cause cell growth and cell death. In this study, we show that cell surface EGFRs promote cell growth, whereas intracellular receptors promote cell death.

This finding that the EGFR when stimulated with a tethered ligand promotes cell growth is consistent with previous reports [34,35]. However, due to the slowed EGFR endocytic trafficking in the MDA-MB-468 cells, we can conclude that the increased growth is due to the spatial localization of the receptor rather than prolonged activation. After 16 hours of stimulation with EGF or EGF-beads, the levels of cell surface and intracellular EGFR tyrosine phosphorylation are comparable, indicating that the duration of receptor signaling can not account for this difference. Inhibition of caspase-3 prevents apoptosis, but offers no growth advantages. Conversely, caspase-3 levels are decreased following EGF-bead stimulation as compared to media alone. Together, these data indicate that cell surface and intracellular receptors stimulate distinct pathways.

Our data indicate that elevated levels of activated EGFR alone are not sufficient to induce apoptosis. Receptor internalization, and likely intracellular accumulation of active receptors, is also necessary. Many cell lines with high levels of EGFRs, either naturally occurring or through exogenous expression, also have slowed endocytic trafficking as measured by the kinetics of degradation of the ligand:receptor complex [26,36]. As a result, when cell lines overexpressing the EGFR are stimulated with EGF, not only are there high levels of activated EGFRs, but the receptors accumulate within the cell due to the slowed rate of receptor degradation. Here we show that despite comparable levels of EGFR phosphorylation, only intracellular receptors induce caspase-3 activity and the induction of apoptosis. It has been demonstrated that apoptotic signaling by the tumor necrosis factor receptor requires the formation of endosomal compartment comprised of the activated receptor and caspase-8 [37]. A “death-inducing signaling complex” may be formed by the activated EGFR in MDA-MB-468 cells.

NIH-PA Author Manuscript

NIH-PA Author Manuscript

NIH-PA Author Manuscript

Spatial regulation of signaling in cancer

These findings could have important implications in the development and treatment of cancers that overexpress EGFR family members. For instance, ErbB2 is expressed in breast cancers that are characterized by enhanced metastatic potential and poor prognosis [38]. ErbB2 does not undergo endocytosis in response to ligand stimulation [39]. When ligand stimulates these receptors to form heterodimers with the EGFR, the active ligand:receptor complex is retained on the plasma membrane. Based on our data, one would predict this cell surface, heterodimeric receptor complex promotes cell growth. Conversely, if the heterodimeric complex could be internalized, that would attenuate cell growth. Evidence that supports this idea comes from data using ErbB2 specific monoclonal antibodies to prevent cell proliferation. It has been reported by Hurwitz et al. only ErbB2 antibodies that induce receptor internalization inhibit tumor growth [40]. Although this observation is consistent with our data, it is premature to know for certain whether to the loss of tumor growth is due to decreased proliferation or increase apoptosis.

There is additional evidence that signaling by the EGFR from the cell surface prevents the induction of cell death. Heparin binding EGF (HB-EGF) is a naturally occurring ligand for the EGFR. The pro-form of HB-EGF is tethered to the plasma membrane and cleavage via a metalloprotease releases the HB-EGF into the extracellular environment. While both proHB-EGF and soluble HB-EGF can stimulate the EGFR [41], only stimulation of kidney epithelial cells with the membrane anchored proHB-EGF protects cells from anoikis and increases cell survival [42].

EGFR Populations

Despite the appearance of comparable levels of EGFR phosphorylation following treatment with EGF and EGF-beads, it is possible that the same receptor population is not being activated. For instance, binding of the EGF-beads may be restricted to EGFRs in a sub-domain of the cell. Based on size, EGF-beads may be sterically excluded from lipid rafts and/or caveolae. Therefore, the EGF-beads can only bind and activate those EGFRs that have been excluded from that cell membrane domain. It has been previously demonstrated the signaling properties of EGFRs localized to caveolae differ from those receptors excluded from the membrane domain, although the molecular mechanism remains controversial [43-45].

A second possibility is that the relative levels of high and low affinity EGFRs may be altered. EGFRs exist in high (K_d = 10-100 pM) and low (Kd = 1-10 nM) affinity states [46], such changes in the nature of the ligand receptor interactions may affect which affinity state is activated. It has been reported that 2-5% of the EGFRs bind EGF with a high affinity, but mediate >95% of the signaling [47-49]. Recent models suggest that the low affinity receptors reflect negative cooperativity in ligand binding. More specifically, the binding of ligand fosters the aggregation of receptors which in turn decreases ligand affinity [50]. Using this model, occupancy of the receptor by the EGF-beads would sterically hinder receptor aggregates from forming maintaining the receptor in a high affinity state. Thus, the differences in signaling mediated by soluble EGF and EGF-beads may reflect which affinity state of the EGFR is activated.

There is precedence in the literature for an association between EGFR affinity state and receptor endocytic trafficking. Ringerike et al. have reported that retention of the EGFR on the cell surface by expression of dominant negative dynamin results in the loss of high affinity EGFRs [11]. Deletion of carboxyl terminal domains of the EGFR that are necessary for receptor endocytosis also cause the loss of high affinity binding [51]. Thus, one of the ways that endocytosis may regulate EGFR signaling is through the conversion of the ligated EGFR from

NIH-PA Author Manuscript

NIH-PA Author Manuscript

NIH-PA Author Manuscript

the more active high-affiinity form to a less active low-affinity form. A more sophisticated analysis of these receptor populations is necessary to make these distinctions.

These data provide a new understanding of how a single receptor can positively and negatively modulate cell physiology. Endocytosis of the EGFR has been widely recognized as an important mechanism for regulating the magnitude and duration of effector activity. Our data provide new evidence that such biochemical changes can alter the cell physiology mediated by the EGFR. Thus, the same receptor can generate opposite effects when at the plasma membrane versus inside the cell.

Supplementary Material

Refer to Web version on PubMed Central for supplementary material.

Acknowledgements

This work was support by The American Cancer Society (RSG-03-021-01), Oklahoma Center for the Advancement of Science and Technology (HR03-014), The Presbyterian Health Foundation, and NIH Grant 5P20RR017703. We thank Drs. Coggeshall, Plafker, and Tsiokas for the assistance in reviewing the manuscript and Dr. George Max for helping with synthesis of the EGF-beads.

References

1. Olayioye MA, Neve RM, Lane HA, Hynes NE. The ErbB Signaling Network: Receptor Heterodimerization in Development and Cancer. EMBO J 2000;19:3159–3167. [PubMed: 10880430]
2. Yarden Y, Sliwkowski MX. Untangling the ErbB Signalling Network. Nat Rev Mol Cell Biol 2001;2:127–137. [PubMed: 11252954]
3. Sorkin A, Waters CM. Endocytosis of growth factor receptors. Bioessays 1993;15:375–382. [PubMed: 8395172]
4. Wiley HS, Burke PM. Regulation of Receptor tyrosine kinase signaling by endocytic trafficking. Traffic 2001;2:557–564.
5. Burke P, Schooler K, Wiley HS. Regulation of Epidermal Growth Factor Receptor Signaling by Endocytosis and Intracellular Trafficking. Mol Biol Cell 2001;12:1897–1910. [PubMed: 11408594]
6. DiGuglielmo GM, Baass PC, Ou WJ, Posner BI, Bergeron JJ. Compartmentalization of Shc, Grb2 and mSOS, and hyperphosphorylation of raf-1 by EGF but not insulin in liver parenchyma. EMBO J 1994;13:4269–4277. [PubMed: 7925272]
7. Ceresa BP, Schmid SL. Regulation of Signal Transduction by Endocytosis. Curr Opin of Cel Bio 2000;12:204–210.
8. Sorkin A, von Zastrow M. Signal Transduction and Endocytosis: Close Encounters of Many Kinds. Nat Cell Biol Rev 2002;3:600–614.
9. Dinneen JL, Ceresa BP. Constitutive activation of rab5 results in a ligand independent redistribution of the EGFR and attenuates its ability to signal. Traffic 2004;5:606–615. [PubMed: 15260830]
10. Huang F, Khvorova A, Marshall W, Sorkin A. Analysis of clathrin-mediated endocytosis of epidermal growth factor receptor by RNA interfernce. J Biol Chem 2004;279:16657–16661. [PubMed: 14985334]
11. Ringerike T, Stang E, Johanessen LE, Sandnes D, Levy FO, Madshus IH. High-affinity binding of epidermal growth factor (EGF) to EGF receptor is disrupted by overexpression of mutant dynamin (K44A). J Biol Chem 1998;273:16639–16642. [PubMed: 9642213]
12. Carpentier JL, Sawano A, Geiger D, Gorden P, Perrelet A, Orci L. Potassium depletion and hypertonic medium reduce “non-coated” and clathrin-coated pit formation, as well as endocytosis through these two gates. J Cell Physiol 1989;138:519–526. [PubMed: 2466853]
13. King AC. Monensin, like methylamine, prevents degradation of 125I-epidermal growth factor, causes intracellular accumulation of receptors and blocks the mitogenic response. Biochem Biophys Res Commun 1984;124:585–591. [PubMed: 6093806]

NIH-PA Author Manuscript NIH-PA Author Manuscript NIH-PA Author Manuscript

14. Armstrong DK, Kaufmann SH, Ottaviano YL, Furuya Y, Buckley JA, Isaacs JT, Davidson NE. Epidermal growth factor-mediated apoptosis of MDA-MB-468 human breast cancer cells. Cancer Res 1994;54:5280–5283. [PubMed: 7923154]
15. Gill GN, Lazar CS. Increase phosphotyrosine content and inhibition of proliferation in EGF-treated A431 cells. Nature 1981;293:305–307. [PubMed: 6268987]
16. Kottke TJ, Blajeski AL, Martins LM, Mesner PW Jr. Davidson NE, Earnshaw WC, Armstrong DK, Kaufmann SH. Comparison of Paclitaxel-, 5-Fluoro-2'-deoxyuridine-, and Epidermal Growth Factor (EGF)-induced Apoptosis. J Biol Chem 1999;274:15927–15936. [PubMed: 10336499]
17. Reynolds AR, Tischer C, Verveer PJ, Rocks O, Bastiaens PIH. EGFR Activation coupled to inhibition of tyrosine phosphatases causes lateral signal propagation. Nat Cell Biol 2003;5:447–453. [PubMed: 12717446]
18. Ceresa BP, Kao AW, Santeler SR, Pessin JE. Regulation of Insulin Receptor Signaling pathways by clathrin mediated endocytosis. Mol Cell Biol 1998;18:3862–3870. [PubMed: 9632770]
19. Ceresa BP, Lotscher M, Schmid SL. Receptor and Membrane Recycling occur with Unaltered kinetics despite dramatic rab5(Q79L)-induced Changes in Endosome geometry. J Biol Chem 2001;276:9649–9654. [PubMed: 11136733]
20. Sorkin AD, Teskenko LV, Nikolsky NN. The endocytosis of epidermal growth factor in A431 cells: a pH of microenvironment and the dynamics of receptor complex dissociation. Exp Cell Res 1988;175:192–205. [PubMed: 2894318]
21. Waters CM, Oberg KC, Carpenter G, Overholser K. Rate constants for binding, dissociation, and internalization of EGF: effect of receptor occupancy and ligand concentration. Biochem 1990;29:3563–3569. [PubMed: 2354152]
22. Schaerli P, Jaggi R. EGF-induced programmed cell death of human mammary carcinoma MDA-MB-468 cells is preceded by activation of AP-1. Cell Mol Life Sci 1998;54:129–138. [PubMed: 9539953]
23. Hansen MB, Nielsen SE, Berg K. Re-examination and further developoment of a precise method for measuring cell growth/cell kill. J. Immunol. Methods 1989;119:203–210. [PubMed: 2470825]
24. Filmus J, Pollak MN, Cailleau R, Buick RN. MDA-468, a human breast cancer cell line with a high number of epidermal growth factor (EGF) receptors, has an amplified EGF receptor gene and is growth inhibited by EGF. Biochem Biophys Res Commun 1985;128:898–905. [PubMed: 2986629]
25. Krupp M, Connolly D, Lane M. Sythnesis, turnover, and down-regulation of epidermal growth factor receptors in human A431 epidermoid carcinoma cells and skin fibroblasts. J Biol Chem 1982;257:11489–11496. [PubMed: 6288686]
26. French AR, Sudlow GP, Wiley HS, Lauffenburger DA. Postendocytic Trafficking of Epidermal Growth Factor-Receptor Complexes is Mediated through Saturable and Specific Endosomal Interactions. J Biol Chem 1994;269:15749–15755. [PubMed: 8195228]
27. Stoscheck CM, Carpenter G. Down regulation of epidermal growth factor receptors: direct demonstration of receptor degradation in human fibroblasts. J Cell Biol 1984;98:1048–1053. [PubMed: 6321514]
28. Dinneen JL, Ceresa BP. Expression of dominant negative rab5 in HeLa cells regulates EGFR endocytic trafficking distal from the plasma membrane. Exp Cell Res 2004;294:509–522. [PubMed: 15023538]
29. Verveer PJ, Wouters FS, Reynolds AR, Bastiaens PIH. Quantitative Imaging of Lateral ErbB1 Receptor Signal Propagation in the Plasma Membrane. Science 2000;290:1567–1570. [PubMed: 11090353]
30. Kempiak SJ, Yip S-C, Backer JM, Segall JE. Local signaling by the EGF receptor. J Cell Biol 2003;162:781–787. [PubMed: 12952932]
31. Guilli LF, Palmer KC, Chen YQ, Reddy KB. Epidermal growth factor-induced apoptosis in A431 cells can be reversed by reducing the tyrosine kinase activity. Cell Growth Differ 1996;7:173–178. [PubMed: 8822200]
32. Masui H, Castro L, Mendelsohn J. Consumption of EGF by A431 cells: evidence for receptor recycling. J Cell Biol 1993;120:85–93. [PubMed: 8416997]
33. Holbro T, Civenni G, Hynes NE. The ErbB receptors and their role in cancer progression. Exp Cell Res 2003;284:99–110. [PubMed: 12648469]

NIH-PA Author Manuscript NIH-PA Author Manuscript NIH-PA Author Manuscript

34. Fan VH, Tamama K, Au A, Littrell R, Richardson LB, Wright JW, Wells A, Griffith LG. Tethered epidermal growth factor provides a survival advantage to mesenchymal stem cells. Stem Cells 2007;25:1241–51. [PubMed: 17234993]
35. Ito Y, Li JS, Takahashi T, Imanishi Y, Okabayashi Y, Kido Y, Kasuga M. Enhancement of the mitogenic effect by artificial juxtacrine stimulation using immobilized EGF. J Biochem 1997;121:514–20. [PubMed: 9133620]
36. Wiley HS. Anomalous Binding of Epidermal Growth Factor to A431 Cells Is Due to the Effect of High Receptor Densities and a Saturable Endocytic System. J Cell Biol 1988;1-7:801–810. [PubMed: 3262110]
37. Schneider-Brachert W, Tchikov V, Neumeyer J, Jakob M, Winoto-Morback S, Held-Feindt J, Heinrich M, Merkel O, Ehrenschwender M, Adam D, Mentlein R, Kabelitz D, Schutze S. Compartmentalization of TNF Receptor 1 Signaling: Internalized TNF Receptosomes as Death Signaling Vesicles. Immunity 2004;21:415–428. [PubMed: 15357952]
38. Stern DF. Tyrosine kinase signalliing in breast cancer: ErbB family receptor tyrosine kinases. Breast Cancer Res 2000;2
39. Lotti LV, Di Lazzaro C, Zompetta C, Frati L, Torrisi MR. Surface distribution and internalization of erbB-2 proteins. Exp Cell Res 1992;202:274–280. [PubMed: 1356817]
40. Hurwitz E, Stancovski I, Sela M, Yarden Y. Suppression and promotion of tumor growth by monoclonal antibodies to ErbB-2 differntially correlate with cellular uptake. P.N.A.S 1995;92:3353–3357. [PubMed: 7724565]
41. Singh AB, Tsukada T, Zent R, Harris RC. Membrane-associated HB-EGF modulates HGF-induced cellular responses in MDCK cells. J Cell Sci 2004;117:1365–1379. [PubMed: 14996914]
42. Singh AB, Sugimoto K, Harris RC. Juxtacrine activation of epidermal growth factor (EGF) receptor by membrane-anchored heparin-binding EGF-like growth factor protects cells from anoikis while maintinaing an epithelial phenotype. J Biol Chem 2007;282:32890–32901. [PubMed: 17848576]
43. Engelman JA, Chu C, Lin A, Jo H, Ikezu T, Okamoto T, Kohtz DS, Lisanti MP. Caveolin-mediated regulation of signaling along the p42/44 MAP kinase cascade in vivo. FEBS Letters 1998;428
44. Mineo C, Gill GN, Anderson RG. Regulated Migration of Epidermal Growth Factor Receptor from Caveolae. J Biol Chem 1999;274:30636–30643. [PubMed: 10521449]
45. Waugh MG, Lawson D, Hsuan JJ. Epidermal Growth Factor Receptor Activation is Localized within Low-bouyant Density, Non-caveolar Membrane Domains. Biochem J 1999;337:591–597. [PubMed: 9895306]
46. Lax I, Bellot F, Howk R, Ullrich A, Givol D, Schlessinger J. Functional analysis of the ligand binding site of EGF-receptor utilizing chimeric chicken/human receptor molecules. EMBO J 1989;8:421–427. [PubMed: 2785915]
47. Bellot F, Moolenaar WH, Kris R, Mirakhur B, Verlaan I, Ullrich A, Schlessinger J, Felder S. High-Affinity Epidermal Growth Factor Binding Is Specifically Reduced by a Monoclonal Antibody, and Appears Necessary for Early Responses. J Cell Biol 1990;110:491–502. [PubMed: 2298813]
48. Defize LHK, Boonstra J, Meisenhelder J, Kruijer W, Tertoolen LGJ, Tilly BC, Hunter T, van Bergen en Henegouwen PMP, Moolenaar WH, de Laat SW. Signal Transduction by Epidermal Growth Factor Occurs Through the Subclass of High Affinity Receptors. J Cell Biol 1989;109:2495–2507. [PubMed: 2553748]
49. Ullrich A, Schlessinger J. Signal transduction by receptors with tyrosine kinase activity. Cell 1990;61:203–212. [PubMed: 2158859]
50. Macdonald JL, Pike LJ. Heterogeneity in EGF-binding affinities arises from negative cooperativity in an aggregating system. Proc Natl Acad Sci U S A 2008;105:112–7. [PubMed: 18165319]
51. Livneh E, Prywes R, Kashles O, Reiss N, Sasson I, Mory Y, Ullrich A, Schlessinger J. Reconstitution of human epidermal growth factor receptors and its deletion mutants in cultured hamster cells. J Biol Chem 1986;261:12490–12497. [PubMed: 3017977]

NIH-PA Author Manuscript

NIH-PA Author Manuscript

NIH-PA Author Manuscript

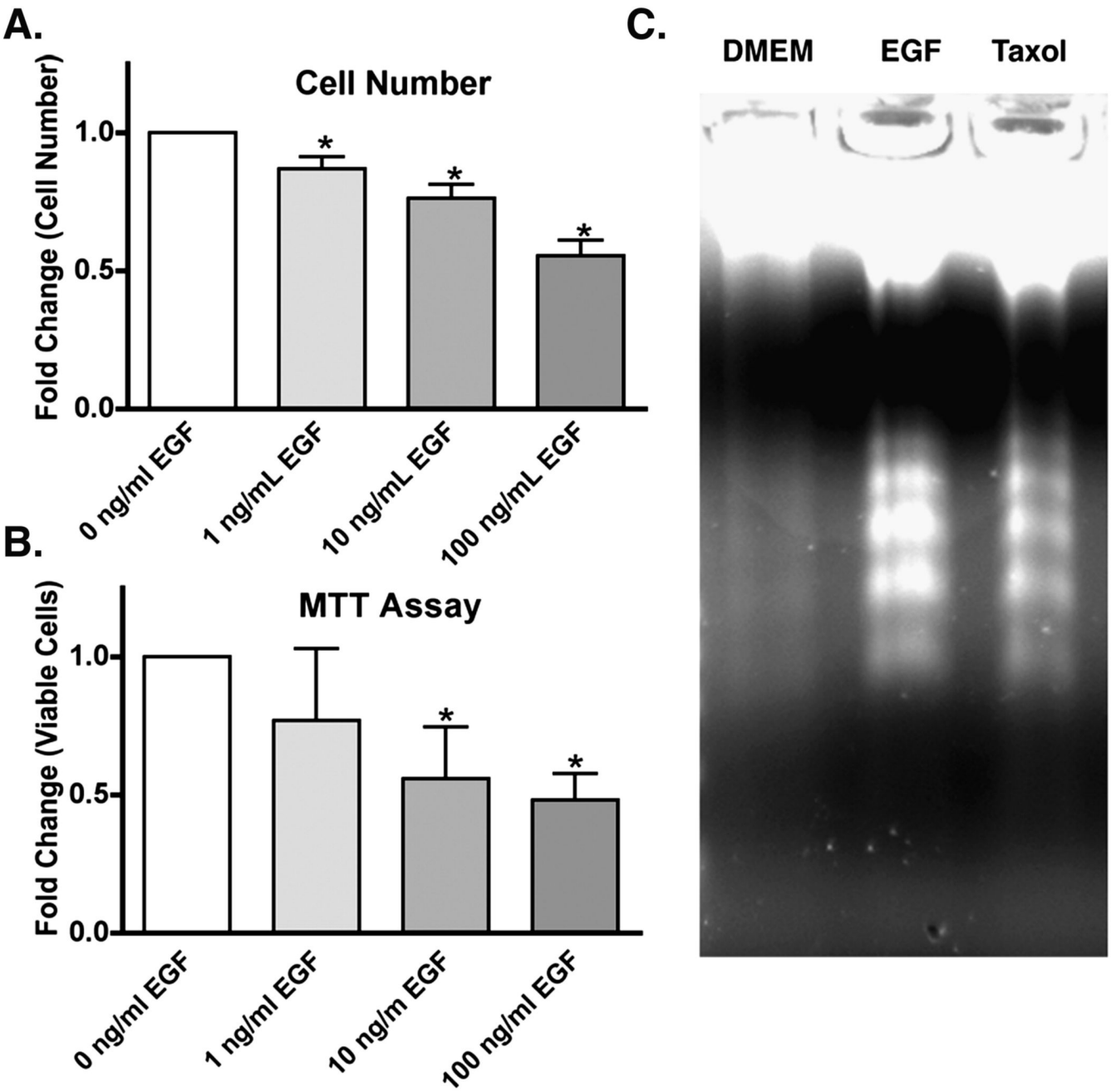

Figure 1. EGF stimulates apoptosis in MDA-MB-468 cells

Serum starved MDA-MB-468 cells were treated with DMEM supplemented with 0-100 ng/ml EGF as indicated. Cell viability was assessed by harvesting cells and counting (A) or MTT assay (B). Data are plotted as the average ± S.E.M. (n=3-4). * Indicates $p < 0.05$ (student's t-test) as compared to 0 ng/ml EGF. E) Genomic DNA was collected from MDA-MB-468 cells treated for 16 hours with 0 ng/ml (DMEM), 100 ng/ml EGF, or 2 μM Taxol as indicated. DNA was run on a 1.2% agarose gel and stained with ethidium bromide.

NIH-PA Author Manuscript

NIH-PA Author Manuscript

NIH-PA Author Manuscript

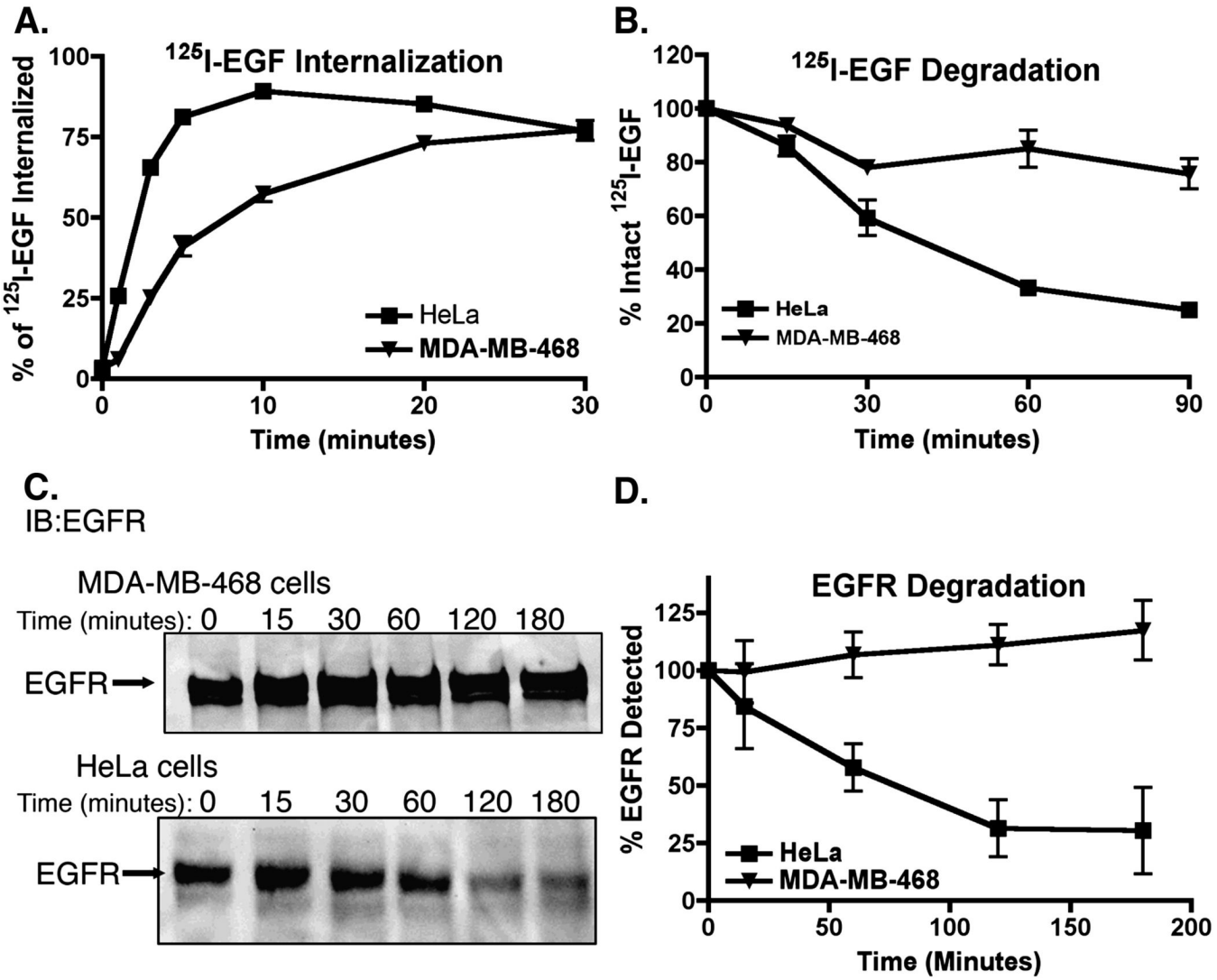

Figure 2. EGFR endocytic trafficking is slowed in MDA-MB-468 cells

A. MDA-MB468 and HeLa cells were incubated with [^{125}I]-EGF for 2 hours on ice to achieve steady-state binding. After the removal of free radioligand, pre-warmed media (37°C) was added to the cells and they were placed at 37°C for the indicated amounts of time. Cell surface ligand was collected by incubation in high salt/low pH buffer (0.5M NaCl/0.2 M acetic acid pH 2.8); internalized radioligand was obtained by solubilizing the remaining cells in 1M NaOH. Radioactivity in each fraction was determined by counting on a Beckman Gamma counter. Data are plotted as the percentage of [^{125}I]-EGF internalized/ (internalized + cell surface). Data shown are the average ± S.E.M. (n=3) B. MDA-MB-468 and HeLa cells were incubated with [^{125}I]-EGF at 37°C for 7.5 minutes followed by extensive washing to remove extracellular and unbound radioligand. At the indicated time points, intact [^{125}I]-EGF was precipitated by trichloroacetic acid. Data are plotted as the average ± S.E.M. percentage of intact [^{125}I]-EGF remaining in the cell at each time point (n=3). C. MDA-MB-468 cells and HeLa cells were treated with 100 ng/ml EGF for the indicated times. Cell lysates were collected, resolved by 7.5% SDS-PAGE, and immunoblotted for the EGFR. Shown is a representative blot repeated three times. D. Quantification of three experiments as performed in B. Data are plotted as the

relative level of EGF at each time point. The data are the average ± S.E.M. from three experiments.

NIH-PA Author Manuscript

NIH-PA Author Manuscript

NIH-PA Author Manuscript

NIH-PA Author Manuscript

NIH-PA Author Manuscript

NIH-PA Author Manuscript

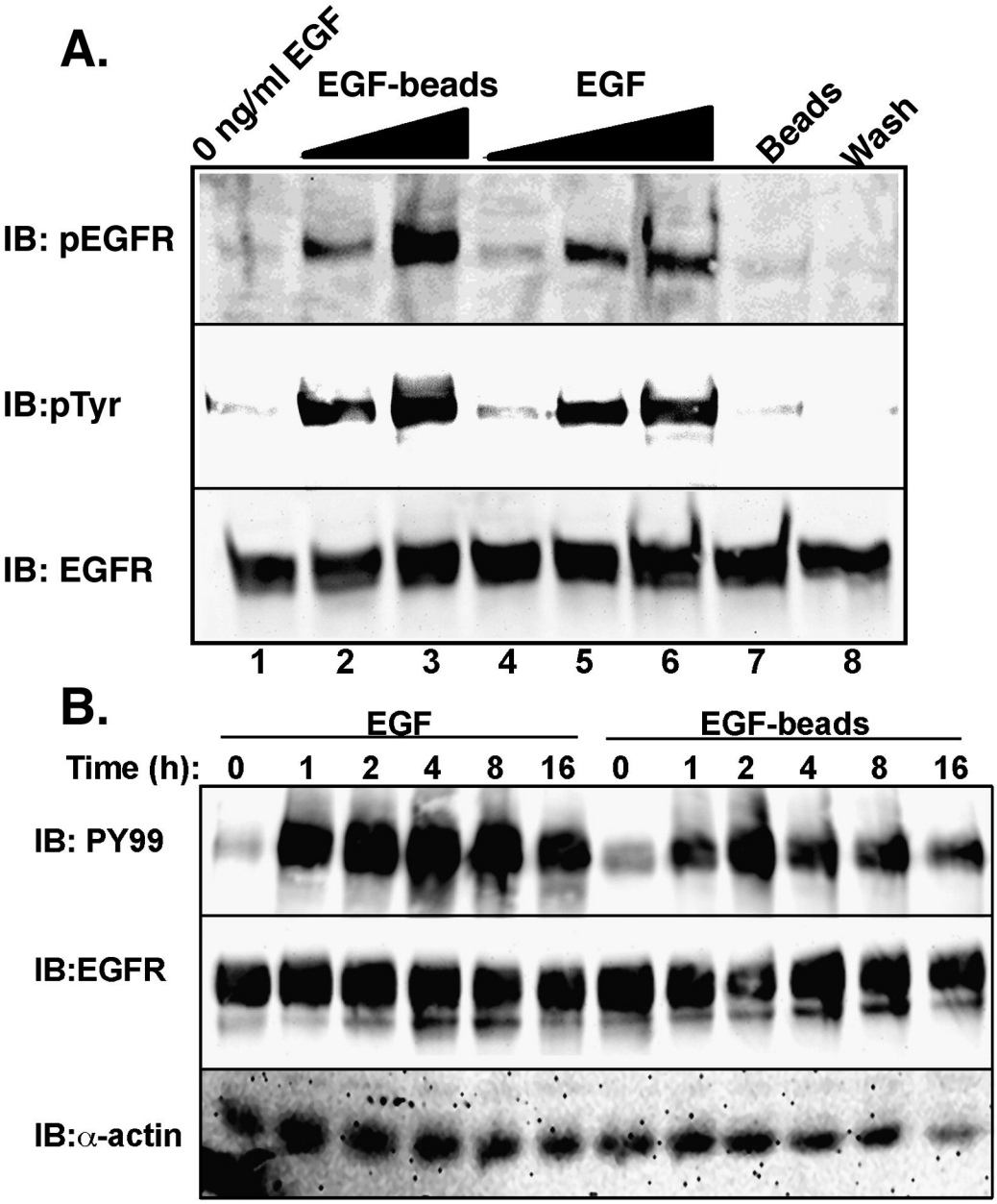

Figure 3. EGF-beads can stimulate the EGFR

A. Serum starved MDA-MB-468 cells were treated for 1 hour with 1) DMEM, 2) ~1 ×10^9/ml EGF-Beads 3) ~2 ×10^9/ml EGF-Beads, 4) 1 ng/ml EGF, 5) 10 ng/ml EGF, 6) 100 ng/ml EGF, 7) ~1 × 10^9 polystyrene beads/ml (Beads), or 8) 40 μL of the final wash (Wash) in the EGF-bead synthesis (all in DMEM). Cells were lysed, cellular protein was separated by 7.5% SDS-PAGE, transferred to nitrocellulose, then probed with antibodies against phosphorylated EGFR, phosphotyrosine, EGFR, α-actin. B. Cells were treated with EGF (100 ng/ml) or ~1 × 10^9 EGF-beads/ml for 0, 1, 2, 4, 8, 16 hours at 37°C. Cell lysates were prepared and probed with either an anti-phosphotyrosine (PY99) or anti-EGFR antibody.

NIH-PA Author Manuscript

NIH-PA Author Manuscript

NIH-PA Author Manuscript

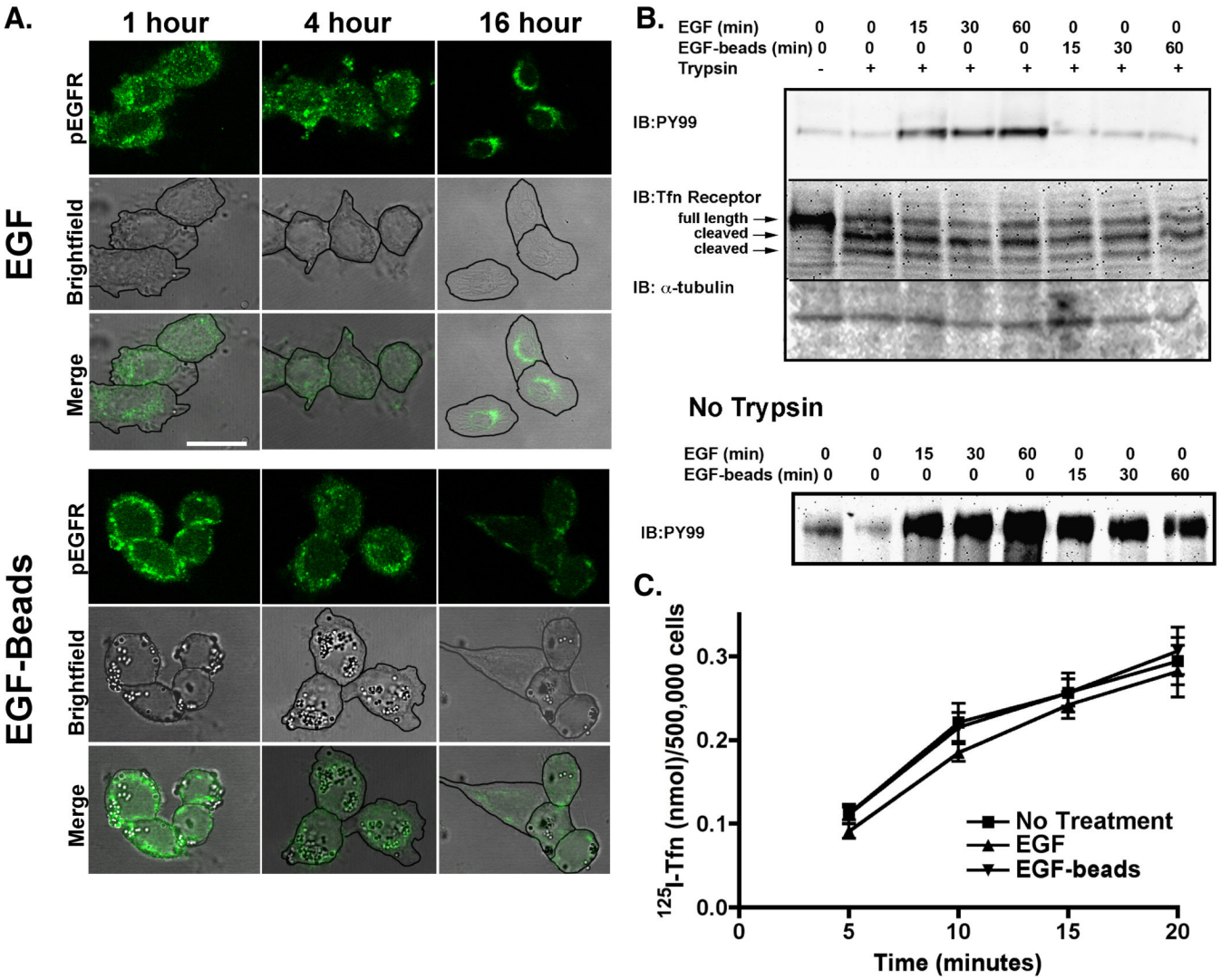

Figure 4. EGF-beads retain the activated EGFR on the cell surface

A. MDA-MB-468 cells were treated with either 100 ng/ml EGF or ~ 1 ×10^9 EGF-beads/ml, as indicated, for 1, 4, or 16 hours at 37°C. Cells were fixed and processed for indirect immunofluorescence using an antibody against the phosphorylated EGFR (Cell Signaling) followed by incubation with an Alexa488-conjugated goat anti-mouse secondary antibody. Images were collected using a Leica TCS NT confocal microscope. Shown are representative sections of the middle of the cell from an experiment repeated three times. Fluorescent (pEGFR) and brightfield images were collected of the same cells. The periphery of the cell was marked using Adobe Photoshop and the two images were merge to indicate the relative distribution of the the fluorescent labeling. Size bar is 20 μm. B. Serum starved MDA-MB-468 cells were treated with DMEM, 100 ng/ml EGF, or ~1 × 10^9 EGF-Beads/ml for the indicated times. After ligand treatment, the cells were treated with or without trypsin as indicated (see Experimental Procedures). Cell lysates were prepared, separated by 7.5% SDS-PAGE, transferred to nitrocellulose, then probed with antibodies against phosphotyrosine (PY99), transferrin, and α-tubule (upper panels). Parallel samples were treated with ligand, but not subjected to trypsinization and probed with an anti-phosphotyrosine antibody (PY99) to indicate receptor activity. Shown is a representative experiment that was repeated three times. C. Cells were treated with nothing, EGF (100 ng/ml), or EGF-beads (~1 ×10^9/ml) for 1 hour

at 37°C and then incubated with [^{125}I]-transferrin at 37°C for 5-10 minutes. Cell associated [^{125}I]-Tfn was measured as described in Experimental Procedures. Data are plotted as the average ± S.E.M. cell associated [^{125}I]-Tfn (nmoles/500,000 cells) at each time point (n=3).

NIH-PA Author Manuscript
NIH-PA Author Manuscript
NIH-PA Author Manuscript

NIH-PA Author Manuscript

NIH-PA Author Manuscript

NIH-PA Author Manuscript

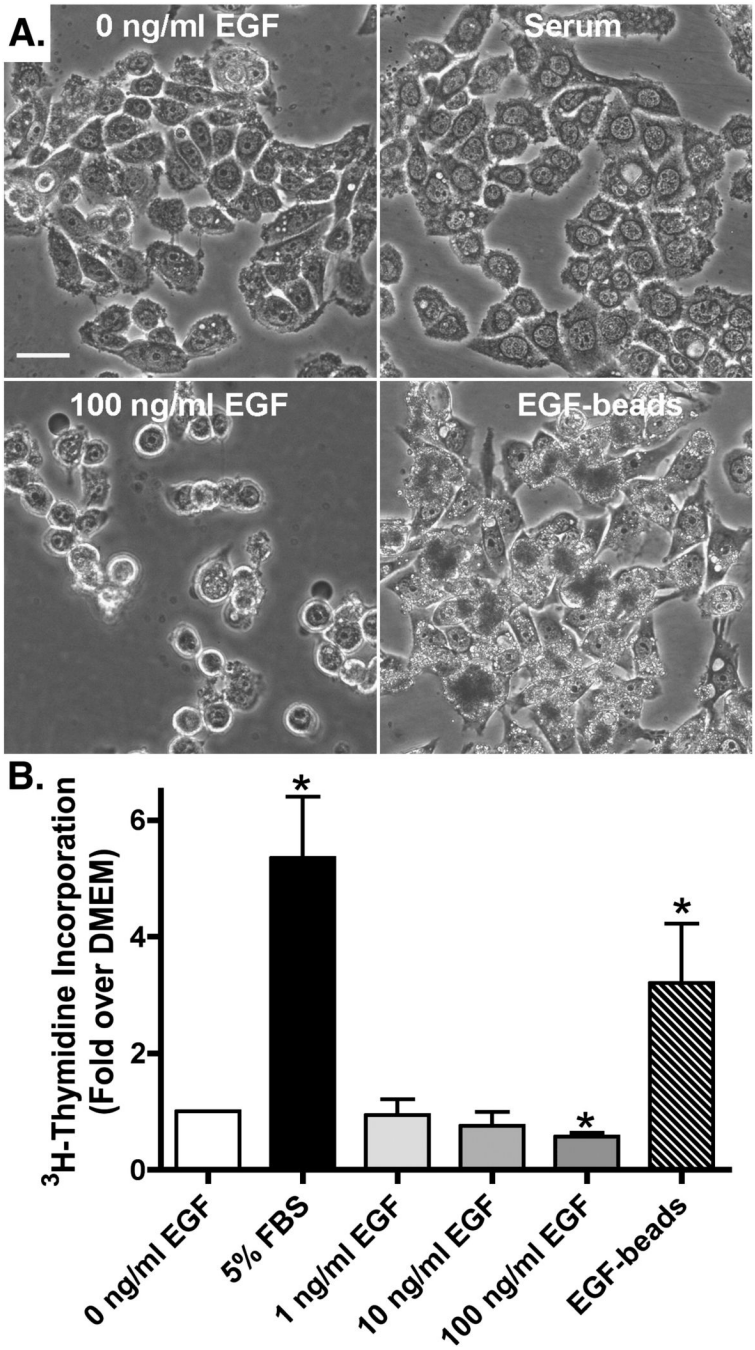

Figure 5. EGF-beads, but not EGF, promote cell growth and not apoptosis

A. MDA-MB-468 cells were incubated for 16 hours with 0 ng/ml EGF (DMEM), 5% FBS (Serum), or DMEM supplemented with 100 ng/ml EGF or ~1 ×10^9 EGF-beads/ml (EGF-beads). Images of cells were collected by light microscopy using a Nikon TE-2000 microscopy and Openlab software. Size bar = 25 μm B. MDA-MB-468 cells were incubated for 16 hours with 0 ng/ml EGF (DMEM), 5% FBS, or DMEM supplemented with 1-100 ng/ml EGF, or ~1 ×10^9 EGF-beads/ml (EGF-beads) for 16 hours in the presence [^{3}H]-thymidine (described Experimental Procedures). Shown is the average ± S.E.M. fold increase in [^{3}H]-thymidine incorporation relative to DMEM treated cells (n=3). * Indicates $p < 0.05$ (student's t-test) as compared to 0 ng/ml EGF.

NIH-PA Author Manuscript

NIH-PA Author Manuscript

NIH-PA Author Manuscript

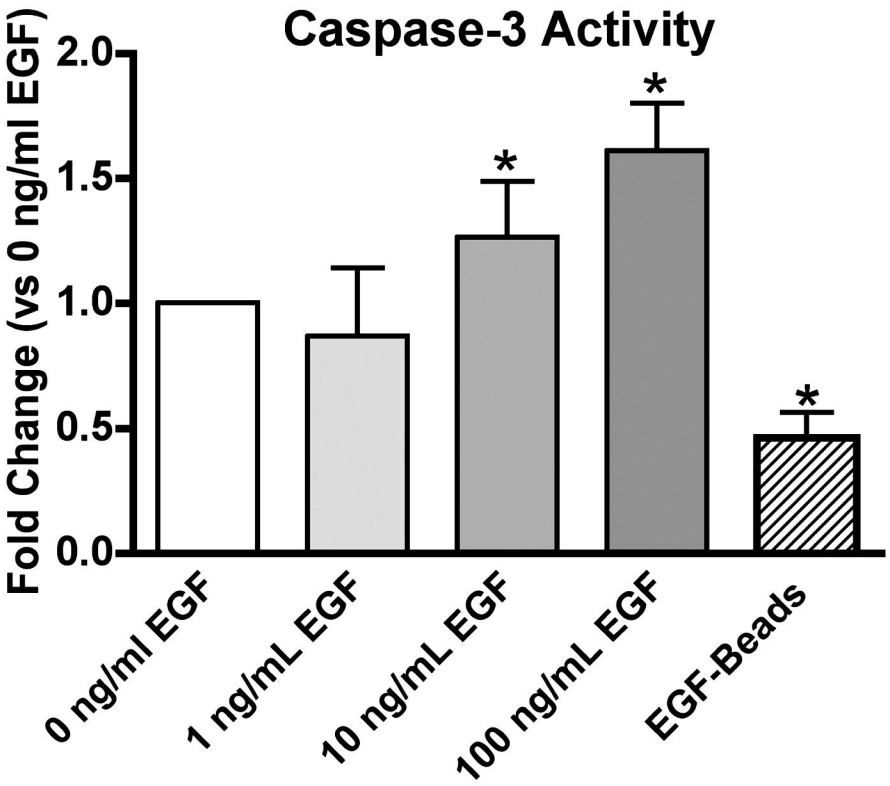

Figure 6. EGF, but not EGF-beads, activates caspase-3

MDA-MB-468 cells were incubated for 16 hours with 0 ng/ml EGF (DMEM), or DMEM supplemented with 1-100 ng/ml EGF, or ~1 $\times 10^9$ EGF-beads/ml (EGF-beads) for 16 hours and assayed for caspase-3 activity (Enz-Chek® Caspase-3 Kit, Molecular Probes, Eugene, OR). Data were normalized to 0 ng/ml EGF and plotted as the average ± S.E.M. (n=3). * Indicates $p < 0.05$ (student's t-test) as compared to 0 ng/ml EGF.

NIH-PA Author Manuscript

NIH-PA Author Manuscript

NIH-PA Author Manuscript

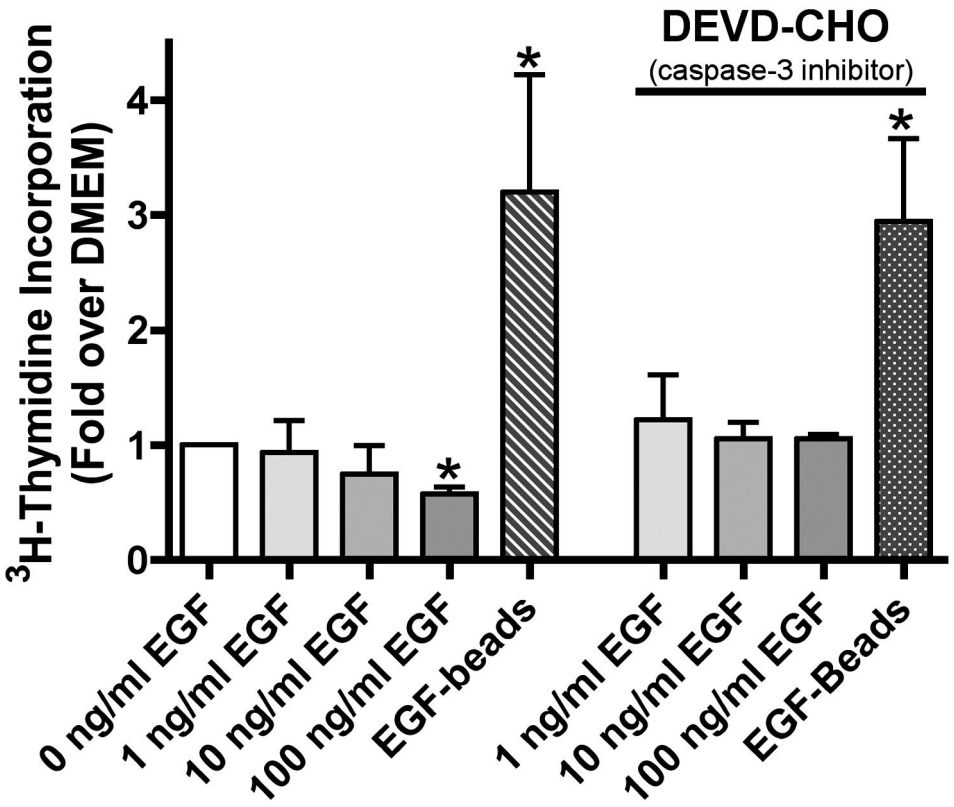

Figure 7. Stimulation of caspase-3 activity by intracellular EGFRs is required to induce apoptosis

Serum starved MDA-MB-468 cells were treated with nothing or the caspase-3 inhibitor DEVDCHO (10 mM) for 1 hour prior to 16 hours of treatment with 0-100 ng/ml EGF or 1 $\times 10^9$ EGF-beads/ml. [^{3}H]-thymidine incorporation was measured. Data are plotted as the average ± S.E.M. (n=3) of the [^{3}H]-thymidine incorporation relative to DMEM. * Indicates $p < 0.05$ (student's t-test) as compared to 0 ng/ml EGF.

NIH-PA Author Manuscript

NIH-PA Author Manuscript

NIH-PA Author Manuscript

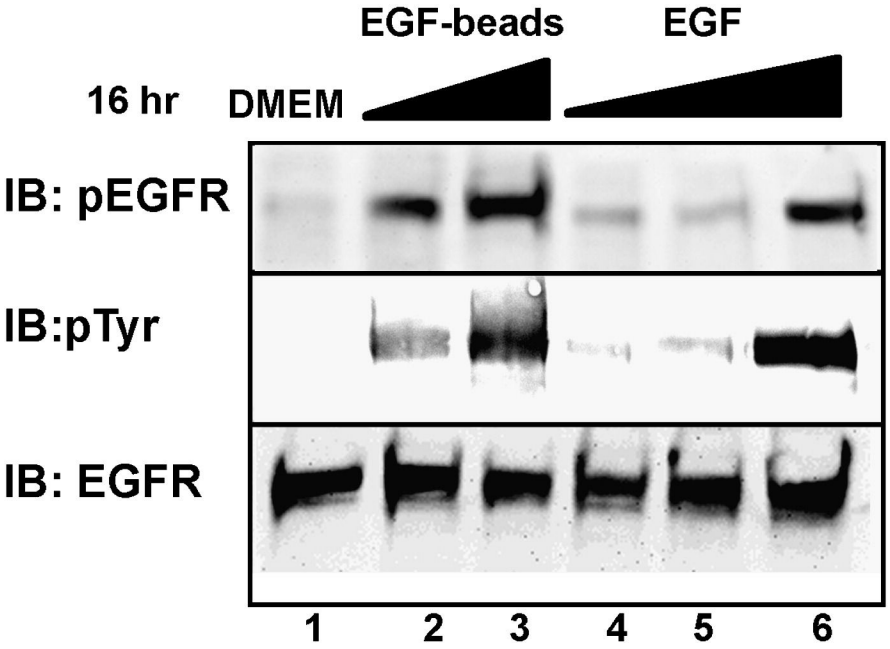

Figure 8. Differences in EGFR signaling are not due to the duration of the signal

Serum starved MDA-MB-468 cells were incubated in 1) 0 ng/ml EGF, 2) ~1 ×10^9 EGF-Beads 3) ~2 ×10^9 EGF-Beads, 4) 1 ng/ml EGF, 5) 10 ng/ml EGF, or 6) 100 ng/ml EGF. Cell lysates were prepared and resolved by 7.5% SDS-PAGE and immunoblotted using antibodies against phosphorylated EGFR, phosphotyrosine, or total EGFR. Shown in a representative experiment repeated three times.